ORIGINAL ARTICLE

Striatal connectivity in pre-manifest Huntington's disease is differentially affected by disease burden

L. Pini[a], K. Youssov[b,c,d,e], F. Sambataro[a], A.-C. Bachoud-Levi[b,c,d,e], A. Vallesi[a,f,*] and C. Jacquemot[b,c,d,*]

[a]*Department of Neuroscience & Padova Neuroscience Center, University of Padova, Padova, Italy;* [b]*Département d'Études Cognitives, École Normale Supérieure, PSL University, Paris;* [c]*Faculté de Santé, Université Paris-Est Créteil, Créteil;* [d]*Inserm U955, Equipe E01 NeuroPsychologie Interventionnelle, Institut Mondor de Recherche Biomédicale, Créteil;* [e]*Centre de référence Maladie de Huntington, Service de Neurologie, Hôpital Henri Mondor, AP-HP, Créteil, France; and* [f]*Brain Imaging and Neural Dynamics Research Group, IRCCS San Camillo Hospital, Venice, Italy*

Keywords:
brain connectivity, disease burden, Huntington's disease, striatum

Received 13 April 2020
Accepted 25 June 2020

European Journal of Neurology 2020, **27:** 2147–2157

doi:10.1111/ene.14423

Background and purpose: Different amounts of cumulative exposure to the toxic mutant form of the huntingtin protein might underlie the distinctive pattern of striatal connectivity in pre-manifest Huntington's disease (pre-HD). The aim of this study was to investigate disease-burden-dependent cortical-striatal and subcortical-striatal loops at different pre-HD stages.

Methods: A total of 16 participants with pre-HD and 25 controls underwent magnetic resonance imaging to investigate striatal structural and functional connectivity (FC). Individuals with pre-HD were stratified into far-from-onset and close-to-onset disease groups according to the disease-burden score. Cortical-striatal and subcortical-striatal FC was investigated through seed-region of interest (ROI) and ROI-to-ROI approaches, respectively. The integrity of white-matter pathways originating from striatal seeds was investigated through probabilistic tractography.

Results: In far-from-onset pre-HD, the left caudate nucleus showed cortical increased FC in brain regions overlapping with the default mode network and increased coupling connectivity with the bilateral thalamus. By contrast, close-to-onset individuals showed increased fractional anisotropy (and mean diffusivity) in the right caudate nucleus and widespread striatal atrophy. Finally, we reported an association between cortical-caudate FC and caudate structural connectivity, although this did not survive multiple comparison correction.

Conclusions: Functional reorganization of the caudate nucleus might underlie plasticity compensatory mechanisms that recede as individuals with pre-HD approach clinical symptom onset and neurodegeneration.

Introduction

Huntington's disease (HD) is an autosomal genetic disorder caused by a pathological expansion of the cytosine-adenine-guanine (CAG) repeat in the huntingtin gene, leading to a mutant form of the huntingtin protein (mHTT). This mutation is responsible for the progressive functional disability [1]. Mutation gene carriers exhibit subtle cognitive deficits and brain alterations before the clinical diagnosis of the disease [i.e. pre-manifest HD (pre-HD)] [2]. Striatal atrophy can be observed up to 10 years before diagnosis in pre-HD [3]. However, individuals with pre-HD are able to maintain a normal level of cognitive functioning to perform usual activities of daily living [2], suggesting that compensatory mechanisms occur over time [4]. Recently, studies investigating brain functional connectivity (FC) through resting-state functional magnetic resonance imaging suggested a compensation model in pre-HD, through an initial

Correspondence: L. Pini, Department of Neuroscience, University of Padova, Via Giustiniani 5, 35128 Padova, Italy (tel.: 049 8213989; fax: 049.8218962; e-mail: pini.lorenzo2@gmail.com).
*A. Vallesi and C. Jacquemot contributed equally to this work.

EUROPEAN JOURNAL OF NEUROLOGY

increase in cortical connectivity and subsequent decline. According to this model, the reduction of gray matter will lead to elevated cortical connectivity, which in turn will give rise to stable behavioral performances [5,6]. These mechanisms have also been reported in several neurodegenerative diseases, such as Alzheimer's disease and frontotemporal dementia. Specifically, compensatory responses have been linked to increased brain connectivity in pre-clinical/mild stages, when brain functional organization might be relatively resilient to the incoming structural damage [7–9]. By contrast, progressive degeneration in the Alzheimer's disease/frontotemporal dementia continuum is associated with an early breakdown of functional connections, related to disease severity [10,11].

Similarly, stage-dependent increased FC was observed in the HD continuum, suggesting early compensatory mechanisms to counterbalance the incoming neurodegeneration [12]. Indeed, the pre-HD stage refers to a heterogeneous stage reflecting non-linear longitudinal changes in brain connectivity in the presence of linear neuronal degeneration [6]. Recently, several studies stratified pre-HD into close to onset or far from onset according to the disease burden score (DBS), an index conveying the toxicity exposure to the mHTT protein [13], reporting disease burden-dependent reorganization of brain connectivity pathways [14]. However, although the striatum represents a core brain region for this pathology, few studies have investigated striatal connectivity across pre-HD stages, reporting contrasting results. Gorges *et al.* [15] investigated caudate connectivity in far-from-onset pre-HD compared with controls reporting null results. By contrast, Kronenbuerger *et al.* [16] reported FC alterations between the striatum and several cortical areas in both close-to-onset and far-from-onset pre-HD. Therefore, it is still unclear whether the striatum might represent a key gate for compensatory mechanisms and at what stage within the pre-HD continuum. To date, no studies have investigated whether subcortical-striatal circuitries are differentially affected within different pre-HD stages.

In this study, we investigated cortical-striatal and subcortical-striatal loops in individuals with close-to-onset and far-from-onset pre-HD. We assumed a dynamic adaptation of striatal FC among different pre-HD stages, showing increased striatal connectivity in the earliest stage but reversing the directionality in close-to-onset pre-HD, as neurodegeneration becomes evident. We expected to report a significant association between structural and FC, confirming compensatory mechanisms overcoming neurodegeneration.

Methods

Participants

We recruited 41 participants between May 2015 and July 2017. A total of 16 were HD mutation gene carriers evaluated with the Unified Huntington's Disease Rating Scale [17]. They were at the pre-HD stage, reporting a total functional capacity score of 13 and a total motor score below 5 [18]. The composite Unified Huntington's Disease Rating Scale (cUHDRS) score, which combines total functional capacity, total motor score, symbol digit modality test and the Stroop word reading test, was also computed [19]. A total of 25 participants were healthy controls (HCs). Participants had no neurological or psychiatric disorders other than HD in the mutation carriers.

Participants with pre-HD were stratified into far-from-onset and close-to-onset groups based on the group median split of the DBS, computed as CAG × age product = [(age at magnetic resonance imaging) × (CAG repeats – 35.5)], which is a validated index of disease burden in pre-HD [13].

This study was performed in accordance with the Declaration of Helsinki. Participants were recruited from an observational clinical biomarker study (NCT01412125) in outpatients approved by the ethics committee of Henri Mondor Hospital (Créteil, France). All participants gave written informed consent and were tested at Henri Mondor Hospital and at the Center for NeuroImaging Research (CENIR, Paris, France).

Magnetic resonance imaging data acquisition and analysis

Participants underwent magnetic resonance imaging on a Prisma 3-T scanner at CENIR (Siemens Medical Solutions, Erlangen, Germany), including eyes-closed resting-state functional magnetic resonance imaging, diffusion and structural scans. The magnetic resonance imaging protocol is described in Appendix S1.

Structural data were processed using FreeSurfer 6.0 (http://surfer.nmr.mgh.harvard.edu/). Subcortical volumetric analysis was limited to the bilateral caudate nucleus, putamen and nucleus accumbens. These structures were normalized to the subject's intracranial volume (ICV) using the following formula: volume norm = volume raw × group mean ICV/subject ICV (in mm^3). Additionally, we investigated both cortical thickness and whole-brain volumetric alterations (see Appendix S1).

A probabilistic tractography approach to reconstruct striatal white-matter pathways was performed using the FMRIB Diffusion Toolbox 3.0 (https://fsl.fmrib.ox.ac.uk/fsl/fslwiki/FDT). The analysis was

focused on fiber bundles starting from each striatal region of interest (ROI) and terminating within the cortex, without using *a-priori* masks. Fractional anisotropy (FA) values within striatal structural pathways were computed. FC analysis was focused on the caudate nucleus, putamen and nucleus accumbens, bilaterally and based on the corresponding FreeSurfer segmentation.

Two different approaches using the Conn toolbox [20] were implemented to investigate both cortical-striatal and subcortical-striatal FC. For detailed description of pre-processing and analysis steps of structural and FC, see Appendix S1.

Statistical analysis

Group differences in sociodemographic features and clinical/cognitive outcomes were assessed with Kruskal–Wallis or chi-squared tests, as appropriate ($P < 0.05$). Within each hemisphere, Kruskal–Wallis P values for ROI subcortical atrophy and FA were corrected for multiple comparisons with Bonferroni correction ($n = 3$ striatal ROIs; $P < 0.017$). All of the analyses were performed using the SPSS package release 23.0 (SPSS Inc., Chicago, IL, USA). FA across groups was compared through a voxel-wise ANOVA ('far-from-onset pre-HD vs. HCs', 'close-to-onset pre-HD vs. HCs', 'far-from-onset pre-HD vs. close-to-onset pre-HD') based on permutation testing at a threshold-free cluster enhancement level of $P < 0.05$ corrected for family-wise error (FWE).

To assess surface cortical-striatal FC differences across groups, the following contrasts were performed through a vertex-wise ANOVA test: 'far-from-onset pre-HD vs. HCs', 'close-to-onset pre-HD vs. HCs' and 'far-from-onset pre-HD vs. close-to-onset pre-HD'. The significance threshold for each contrast was set to $P < 0.05$ with a vertex-level false discovery rate correction with a more conservative cluster-level threshold of $P < 0.01$ FWE corrected. An affine approach was then used for mapping surface coordinates in Montreal Neurological Institute space. Subcortical ROI-to-ROI FC results were reported at $P < 0.05$ false discovery rate corrected at the analysis level and FWE at the network level using network-based statistics [21]. To control for motion, the mean frame-wise displacement was included as covariate in all of the analyses.

For each individual and striatal ROI, a mean global cortical-striatal FC map was computed by extracting corresponding network spatial maps on the pooled sample of HCs and individuals with pre-HD. Positive and negative correlational maps were separately assessed through a one-tailed, one-sample t-test ($P < 0.05$ false discovery rate corrected; cluster-level $P < 0.01$ FWE corrected). Positive correlation maps were then used as masks to compute the mean FC.

Finally, a general linear model was used to investigate the interaction effect of DBS severity (far-from-onset and close-to-onset pre-HD) on the mean FC and cUHDRS score for each bilateral striatal ROI. The same model was applied to investigate the interaction effect on the three groups (HCs, far-from-onset pre-HD and close-to-onset pre-HD) on functional and structural connectivity (i.e. mean FC and mean FA) within each bilateral ROI. P values were corrected for multiple comparisons within each hemisphere ($n = 3$ striatal ROIs; $P < 0.017$) to control for type I error with Bonferroni correction.

Results

Based on the median DBS across pre-HD, eight participants were included in the far-from-onset pre-HD group (below the DBS median) and eight individuals were included in the close-to-onset pre-HD group (above the DBS median). The pre-HD groups and controls were matched for age (HCs, 44 ± 9 years; far-from-onset pre-HD, 41 ± 14 years; close-to-onset pre-HD, 43 ± 6 years; $P = 0.91$), education years (HCs, 15 ± 2 years; far-from-onset pre-HD, 13 ± 2 years; close-to-onset pre-HD, 16 ± 2 years; $P = 0.09$) and sex ($P = 0.66$) (Table 1). Neither total functional capacity score nor total motor score differed across pre-HD groups ($P > 0.1$) (Table 1). Likewise, symbol digit modality test, Stroop test, verbal fluency and cUHDRS score were similar across groups ($P > 0.5$) (Table 1).

No participant was excluded from the analysis due to segmentation failures. Figure S1 illustrates subcortical ROIs across imaging modalities included in the present analysis.

Group comparison revealed differences across groups in bilateral volume of the caudate nucleus (left, $P = 0.003$; right, $P = 0.002$), putamen (left, $P < 0.001$; right, $P < 0.001$) and nucleus accumbens (left, $P = 0.002$; right, $P = 0.003$) (Table 1; Fig. 1a). Post-hoc analyses revealed reduced subcortical volumes in close-to-onset pre-HD compared only with HCs. All of these differences survived multiple comparison correction. Between-group differences did not reach statistical significance in far-from-onset pre-HD compared with both close-to-onset pre-HD and HCs ($P > 0.05$) (Table 1; Fig. 1a). Results were confirmed by the whole-brain volumetric group analyses (Fig. 1b). Compared with controls, the close-to-onset pre-HD group showed bilateral atrophy limited to the striatum. By contrast, the far-from-onset pre-HD

Table 1 Demographic, genetic and subcortical variables of healthy controls (HCs) and pre-manifest Huntington's disease (pre-HD) groups

Variables	HCs (n = 25)	Far-from-onset pre-HD (n = 8)	Close-to-onset pre-HD (n = 8)	P value
Socio-demographic, clinical and genetic variables				
Age (years)	44 ± 9	41 ± 14	43 ± 6	0.91
Education (years)	15 ± 2	13 ± 2	16 ± 2	0.09
Sex (female)	11	5	4	0.66
Handedness (right)	24	6	7	0.21
Disease burden score	–	224 ± 44	364 ± 43	*0.001*
CAG repeat	–	41 ± 2	44 ± 2	*0.008*
Clinical/cognitive outcomes				
Total functional capacity	–	13 ± 0	13 ± 0	1
Total motor score	–	0 ± 0	0.5 ± 1	0.14
Symbol digit modality test	–	53 ± 13	53 ± 8	1
Stroop (word)	–	103 ± 11	99 ± 2	0.57
Verbal fluency (letters)	–	65 ± 17	66 ± 21	0.94
cUHDRS score [15]	–	17 ± 1	17 ± 1	0.53
Subcortical volumes				
Caudate				
Left	3402 ± 341	3205 ± 509	2498 ± 544*	*0.003*
Right	3570 ± 385	3367 ± 482	2614 ± 535*	*0.002*
Putamen				
Left	5002 ± 529	4652 ± 581	3774 ± 581*	*<0.001*
Right	5045 ± 521	4654 ± 501	3839 ± 498*	*<0.001*
Accumbens				
Left	607 ± 98	543 ± 89	460 ± 86*	*0.002*
Right	561 ± 79	502 ± 71	428 ± 100*	*0.003*

CAG, cytosine-adenine-guanine; cUHDRS, composite Unified Huntington's Disease Rating Scale. Data are given as mean ± SD. $P < 0.05$ are shown in italics. * Statistically different from HCs.

group did not show regions with reduced gray matter compared with both controls and the close-to-onset pre-HD group. Differences between pre-HD groups and increased gray matter in pre-HD groups compared with controls were not found. Similarly, only individuals with close-to-onset pre-HD showed reduced cortical thickness compared with controls, mapping in the superior/middle occipital gyrus (Montreal Neurological Institute; $x = 24$; $y = -86$; $z = 22$) (Fig. 1c). We did not observe differences in cortical thickness between far-from-onset pre-HD and close-to-onset pre-HD and neither did thickness increase among pre-HD groups compared with controls.

Probabilistic tractography showed consistent striatal white-matter pathways across individuals (Fig. S2). Group comparisons did not identify differences in mean FA pathways originating from striatal ROIs (left caudate, $P = 0.28$; right caudate, $P = 0.84$; left putamen, $P = 0.08$; right putamen, $P = 0.65$; left nucleus accumbens, $P = 0.44$; right nucleus accumbens, $P = 0.24$) (Fig. 2a). By contrast, voxel-wise analysis showed increased FA in individuals with close-to-onset pre-HD compared with both HCs and individuals with far-from-onset pre-HD in a small portion of the right caudate streamline (Table S2, Fig. 2b). A *post hoc* analysis demonstrated that increased FA in close-to-onset pre-HD was accompanied by increased mean diffusivity (MD) within the right caudate streamline (Table S2, Fig. S4).

The FC surface maps were spatially different across striatal structures (Table S1 and Fig. S3). Group comparison showed increased FC in the far-from-onset pre-HD group compared with HCs in the left caudate-cortical functional pathway (Fig. 3; Table 2). Specifically, increased connectivity was found within the posterior cingulate/precuneus and right inferior parietal lobe. Similarly, when we compared left caudate nucleus connectivity in individuals with far-from-onset pre-HD vs. close-to-onset pre-HD, in the former group we found increased connectivity in the posterior cingulate/precuneus and inferior parietal lobe, bilaterally (Fig. 3; Table 2). No significant differences were found between individuals with close-to-onset pre-HD and HCs. No differences were reported between pre-HD and controls with regard to FC of the right caudate nucleus, bilateral putamen and bilateral nucleus accumbens. [Correction added on 20 August 2020, after first online publication: This paragraph was moved from the figure legend to the Results section.]

Subcortical ROI-to-ROI analysis showed increased coupling connectivity in individuals with far-from-onset pre-HD compared with HCs between the left

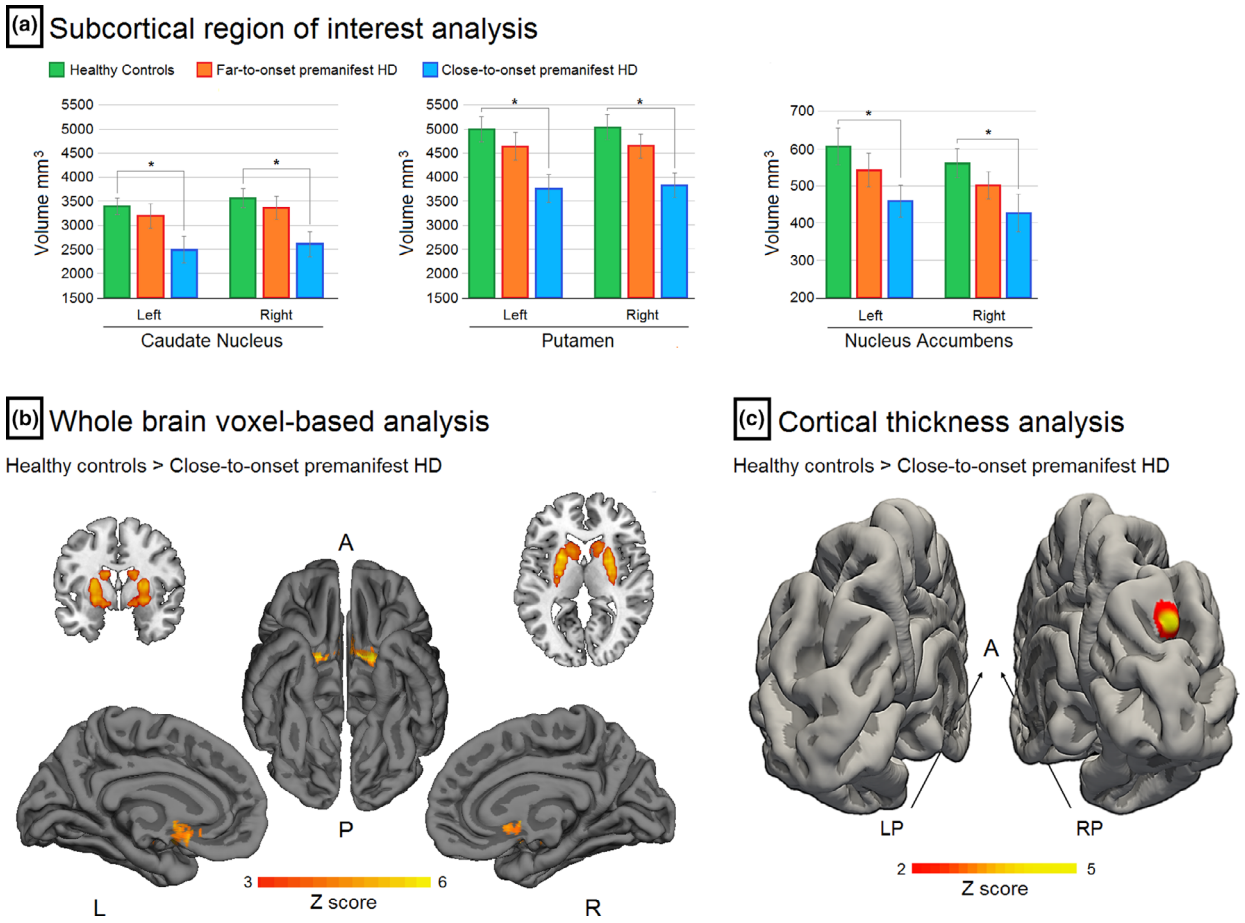

Figure 1 (a) Group volumetric subcortical analysis of caudate nucleus (left panel), putamen (middle panel) and nucleus accumbens (right panel). *Significant differences. (b) Whole-brain voxel-wise analysis. Compared with controls, individuals with close-to-onset pre-manifest Huntington's disease (pre-HD) showed atrophy limited to the striatum, bilaterally. (c) Reduced right middle occipital cortical thickness in close-to-onset pre-HD compared with controls. Green, controls; orange, far-from-onset pre-HD; blue, close-to-onset pre-HD; red/yellow, decreased volume in close-to-onset pre-HD vs. controls. A, anterior; L, left; R, right; P, posterior. [Colour figure can be viewed at wileyonlinelibrary.com]

caudate and bilateral thalamus (Fig. 4). Between-group comparison revealed no significant differences between far-from-onset individuals and controls and across pre-HD groups.

There was no significant interaction between cUHDRS scores and pre-HD groups on mean FC of any striatal ROI (left caudate, $W = 0.658$, $P = 0.42$; right caudate, $W = 0.707$, $P = 0.40$; left putamen, $W = 0.552$, $P = 0.46$; right putamen, $W = 0.683$, $P = 0.41$; left accumbens, $W = 1.16$, $P = 0.28$; right accumbens, $W = 0.009$, $P = 0.93$). [Correction added on 20 August 2020, after first online publication: This paragraph was moved from the figure legend to the Results section.]

Finally, a significant interaction effect was reported in the left caudate nucleus between groups and FA on FC ($W = 7.99$, $P = 0.018$), although this did not survive multiple comparison correction (Fig. S5). No significant interactions were reported for the right caudate nucleus ($W = 2.432$, $P = 0.18$), putamen (left, $W = 0.022$, $P = 0.99$; right, W = 4.021, $P = 0.13$) and nucleus accumbens (left, $W = 0.103$, $P = 0.95$; right, W = 1.330, $P = 0.51$).

Discussion

These findings suggest different patterns of brain reorganization during pre-HD stages, where enhanced caudate nucleus FC is one of the earliest signs of neural reorganization in the pre-HD continuum, a pattern that disappears as the disease progresses and as striatal degeneration becomes evident. Functional reorganization of the caudate nucleus in far-from-onset pre-HD mapped to brain regions showing a consistent pattern of positive connectivity among HCs (Fig. S4). Specifically, brain regions mapping to the default

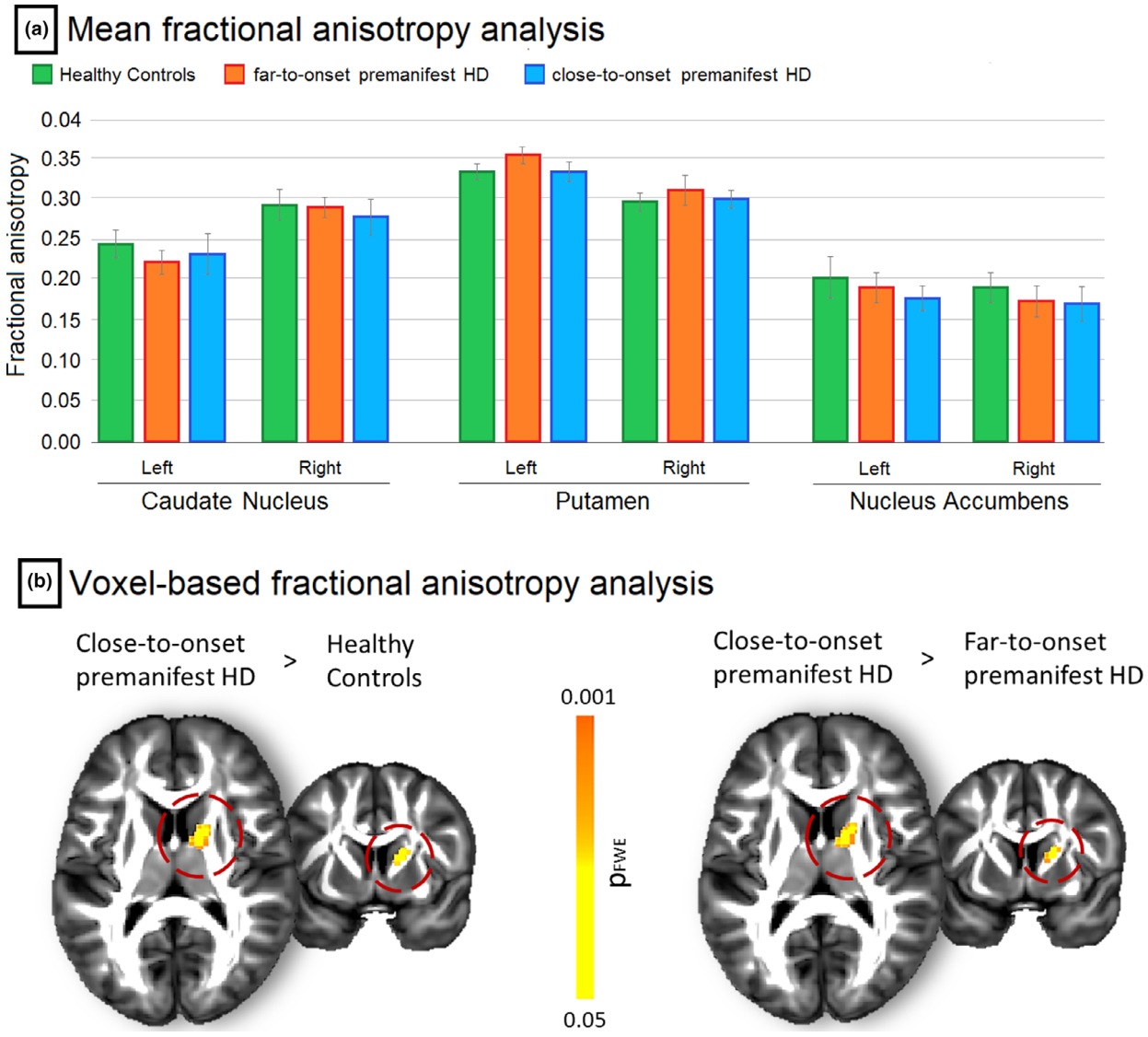

Figure 2 (a) Bilateral striatal fractional anisotropy (FA) in pre-manifest Huntington's disease (pre-HD) groups and healthy controls (HCs). (b) Voxel-wise group analysis within striatal streamlines. Gaussian smoothing (sigma = 1) was applied on the maps for better visualization. Significant clusters are superimposed over the standard-space FA template provided by FSL. Green, HCs; orange, far-from-onset pre-HD; blue, close-to-onset pre-HD; red/yellow, increased FA in close-to-onset pre-HD. [Correction added on 20 August 2020, after first online publication: Figure 2's legend has been updated to move some text to the Results section.]. [Colour figure can be viewed at wileyonlinelibrary.com]

mode network, precuneus and inferior parietal lobe showed increased connectivity in far-from-onset pre-HD. In far-from-onset pre-HD, the left caudate nucleus showed increased FC with the bilateral thalamus. This loop receives cortical inputs that are integrated within the striatum and thalamus before being projected back to the cortex [22]. Increasing evidence suggests that subcortical structures may serve as critical hubs integrating cortical functional networks via a cortical-striato-thalamic loop. The caudate nucleus and thalamus showed functional integration between neural networks supporting attention and the top-down control and default mode network, suggesting that these subcortical regions may act as cognitive integration zones [23]. Taken together, these results might suggest a compensatory interplay between plasticity mechanisms reinforcing pre-existent functional pathways and segregating anticorrelated neuronal processes through a reorganization of the cortical-striato-thalamic loop in far-from-onset pre-HD. This very early compensatory pattern is supported by previous animal studies reporting compensatory

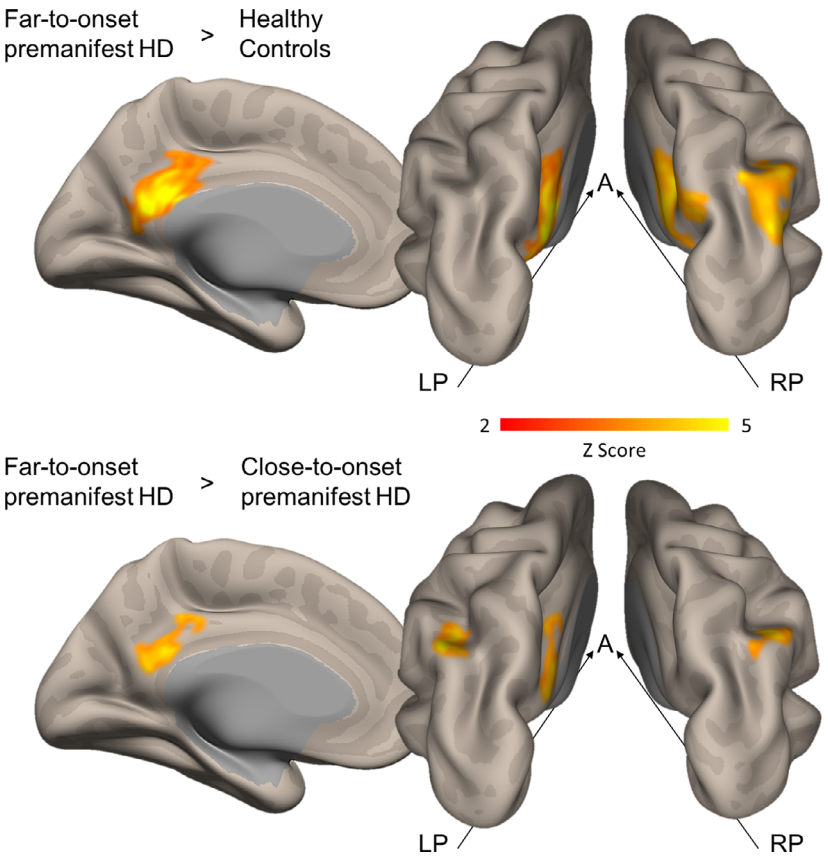

Figure 3 Left caudate-cortical connectivity differences between far-from-onset pre-manifest Huntington's disease (pre-HD) and controls (top panel) and close-to-onset pre-HD (bottom panel). Significant results are superimposed over the Freesurfer cortical template. A, anterior; LP, left-posterior; RP, right-posterior. [Colour figure can be viewed at wileyonlinelibrary.com]

Table 2 Differences in functional connectivity between left caudate and cortical regions in far-from-onset pre-manifest Huntington's disease (pre-HD) compared with healthy controls (HCs) and close-to-onset pre-HD

Region name	Side	Cluster mass	MNI coordinates			p-FWE
			x	*y*	*z*	
Far-from-onset pre-HD > HCs						
Precuneus/PCC	Left	10 283	−3	−52	20	0.009
	Right	18 109	13	−50	38	0.005
Inferior parietal lobe	Right	11 216	38	−79	35	0.008
Far-from-onset pre-HD > close-to-onset pre-HD						
Inferior parietal lobe	Left	5375	−42	−60	48	0.005
	Right	3961	42	−52	44	0.006
Precuneus/PCC	Left	4338	−1	−45	28	0.006

MNI, Montreal Neurological Institute; PCC, posterior cingulate cortex. $P < 0.05$ with a vertex-level false discovery rate correction and a cluster-level threshold of $P < 0.01$ family-wise (p-FWE) error corrected.

mechanisms for the loss of striatal function in pre-HD [24,25]. Recently, Cabanas *et al.* [26] reported a significant increase of neuronal activity in the dorsomedial striatum of pre-HD mice, which disappeared as soon as the motor symptoms became manifest. Similar compensatory mechanisms have been described in preclinical progranulin mutation carriers [9]. However, no significant associations between caudate nucleus FC and cognitive functioning were reported, indirectly supporting the idea that compensation is likely to be effective at the behavioral level.

Changes in connectivity were reported only for the left caudate nucleus, which might suggest a hemispheric asymmetry in very early HD, consistent with previous literature [27,28]. A divergent involvement of the caudate nucleus was confirmed by the voxel-wise FA (and MD) analysis, in line with a recent meta-analysis reporting increased FA in the caudate nucleus of pre-HD (and increased MD in patients with HD) [29]. Currently, there are different interpretations of increased striatal FA in HD. Douaud *et al.* suggested that it expresses a preferential loss of the striatal connections along specific radiating directions, whereas some others are relatively spared, transforming the striatum into a more organized structure [30].

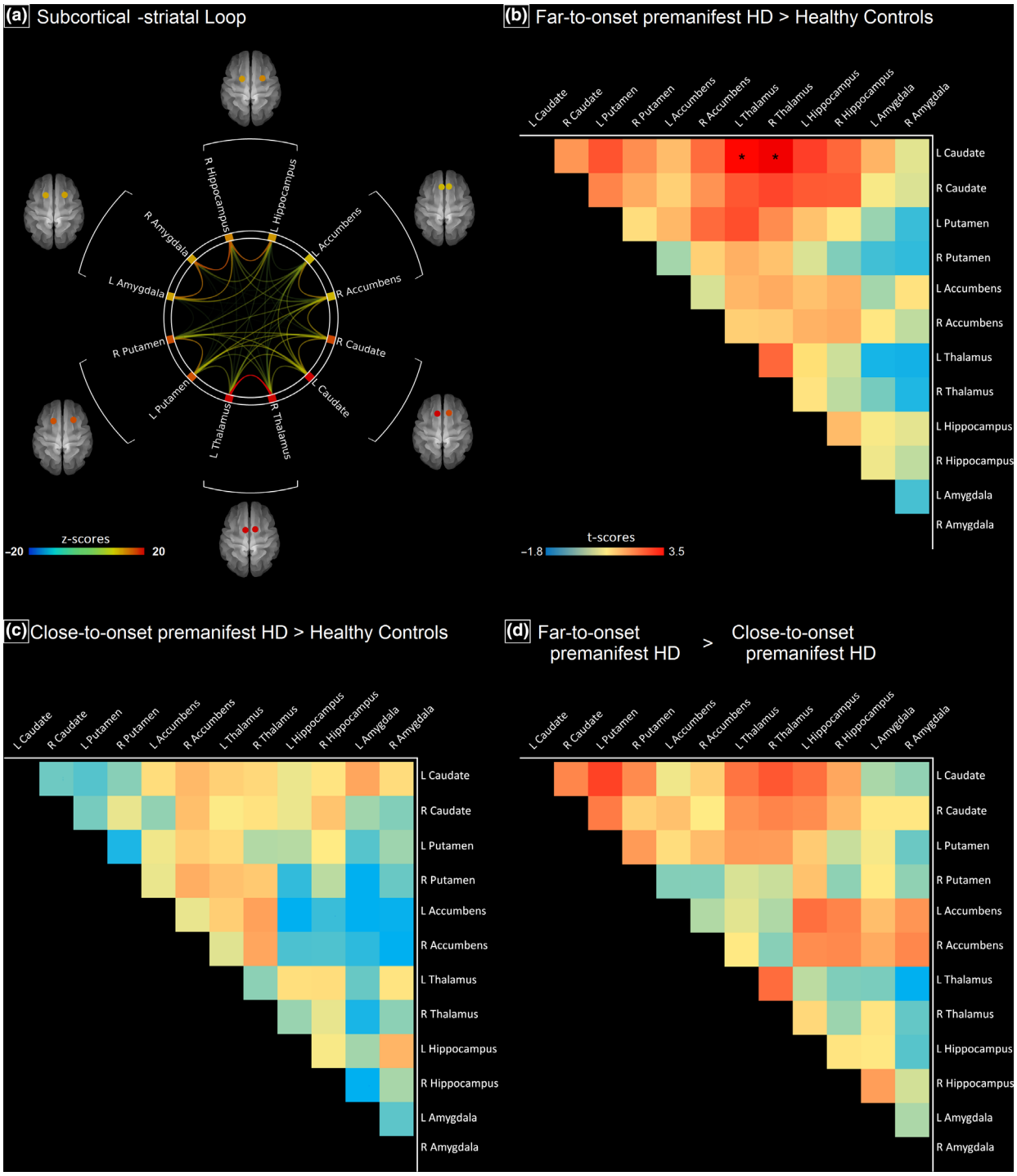

Figure 4 (a) Subcortical-striatal connectivity in the whole sample. (b) Differences in striatal region-to-region functional connectivity between far-from-onset pre-manifest Huntington's disease (pre-HD) vs. healthy controls (HCs). (c) Close-to-onset pre-HD vs. HCs. (d) Far-from-onset pre-HD vs. close-to-onset pre-HD. *Significant differences. L, left; R, right. [Correction added on 20 August 2020, after first online publication: Figure 4's legend has been updated to move some text to the Results section.]. [Colour figure can be viewed at wileyonlinelibrary.com]

Alternatively, it has been suggested that increased FA could result from pathological mechanisms that modify tissue integrity [31]. We found increased FA (and MD) in the right caudate nucleus of close-to-onset pre-HD, which might represent a marker of loss of connections in pre-HD approaching clinical

symptoms, congruent with gray-matter neurodegeneration observed in these individuals. Taken together, these results suggest that increased connectivity of the left caudate nucleus might temporally compensate the very subtle incoming structural damage, whereas the right caudate nucleus might exhibit an early vulnerability (becoming significant in the close-to-onset group), overcoming the functional compensation.

Alternative explanations are also possible. The inclusion of a higher number of right-handed individuals might explain this asymmetry, as the caudate nucleus of the dominant hemisphere might exhibit the maximal dynamic compensatory reorganization. Future studies should investigate striatal connectivity in left-handed individuals with HD to directly address the influence of handedness.

Significant interaction was found between groups for the association between FC and FA of the left caudate nucleus, although this did not survive multiple comparison correction. Specifically, a negative relationship was reported between FC and FA in individuals with far-from-onset pre-HD, whereas the relationship faded out in both HCs and close-to-onset pre-HD ($R^2 < 0.07$). This result may reinforce the assumption of a dynamic reorganization of functional pathways linked with a stage-dependent structural organization of the caudate.

We confirmed previous studies investigating neurodegeneration in close-to-onset pre-HD [32]. The pattern of morphological alterations in close-to-onset pre-HD is congruent with recent data from a meta-analysis reporting volume reduction in the bilateral striatum and right middle occipital gyrus in pre-HD (Fig. 1c) [33]. Although these structural changes in close-to-onset individuals suggest disease progression, we did not find FC reduction, although, as expected, a trend towards reduced subcortical-striatal connectivity was observed. This pattern might suggest that the underlying FC effect of close-to-onset pre-HD is relatively small. If there are subtle effects of close-to-onset pre-HD on FC, these might be detected with larger sample sizes or by improving signal-to-noise ratio. Furthermore, it is also possible that FC in close-to-onset individuals differs in some other brain regions.

Alternative explanations are still possible. The lack of FC differences in close-to-onset pre-HD may suggest that increased cortical-caudate FC is due to aberrant pruning of inhibitory synapses, whereas the excitatory inputs that the striatum receives from the cortex might be spared in the early stage of disease [34]. In individuals with pre-HD closer to clinical symptoms, neurodegeneration may subsequently involve excitatory synapses, restoring the balance between synapses. Zullo *et al.* [35] reported an association between longevity and the activity of genes involved in downregulation of neural excitation. These results might suggest a detrimental effect of the increased caudate-cortical connectivity, which might in turn trigger the clinical symptoms of HD. Future studies should disentangle whether hyper-connectivity is linked with compensatory or maladaptive mechanisms. This information will help to guide new treatments, including brain stimulation interventions aimed to normalize FC [36].

This study has both strengths and limitations. The main strength is that we investigated, for the first time, both cortical-striatal and subcortical-striatal loops in individuals with pre-HD stratified according to the DBS. This design enabled the assessment of specific striatal alterations within different pre-HD stages. Among the limitations, the relatively small sample size of participants limits the generalization of the present findings and prevents examination of the role of potentially modulatory factors, such as handedness. Thus, our results should be considered as exploratory and interpreted with caution. It would be valuable in future to longitudinally assess whether the pattern of increased connectivity would change within subjects as a function of time.

In conclusion, this study suggests early disease-burden-dependent FC reorganization involving the left caudate nucleus in pre-HD. These findings could represent new insights into understanding biomarkers and biological phenotypes linked with genotype, which would help the development of new therapies and treatment outcomes [37].

Acknowledgements

This work was supported by the European Research Council Starting Grant LEX-MEA no. 313692 (FP7/2007-2013) to A.V., ANR-11-JSH2-006-1 grant to C.J., interface contract (INSERM) to A.-C.B.-L. and ANR-17-EURE-0017. The Henri Mondor Hospital National Reference Centre for Huntington's Disease funded the follow-up of all of the patients included in this study (Ministry of Health). We thank Benoit Beranger for his help in data acquisition.

Disclosure of conflicts of interest

The authors declare no financial or other conflicts of interest.

Data availability statement

Both gene carriers and controls signed an informed consent form guaranteeing data confidentiality and we

were therefore unable to share our data through deposition in an open-access repository. However, the data are available from the last author, upon request and for research purposes only. The person requesting the data must sign a confidentiality agreement provided by Assistance Publique-Hôpitaux de Paris stipulating that they will make no attempt to identify the patients. Given the small size of the cohorts studied, identification of the patients from center information is feasible. Thus, even with a signed confidentiality agreement, some of the information will be removed to ensure that the patients cannot be identified.

Supporting Information

Additional Supporting Information may be found in the online version of this article:

Figure S1 Striatal segmentation (upper panel) and white matter pathway tractography (middle panel) in a healthy control displayed on the left hemisphere. Bottom panel shows functional connectivity pattern in the pooled group of controls and pre-manifest HD individuals for the left hemisphere.

Figure S2 Tractography results for the left hemisphere in a subsample of controls (top panel) and pre-manifest Huntington's disease (bottom panel).

Figure S3 Functional connectivity spatial maps for positive and negative correlations between left striatal structures and cortical regions within the healthy control group (one-tailed, one sample *t*-test; $P < 0.05$ with a vertex-level false discovery rate correction and a cluster-level threshold of $P < 0.01$ family-wise error corrected).

Figure S4 Close-to-onset pre-manifest Huntington's disease (pre-HD) compared with both controls (left panel) and far-from-onset pre-HD (right panel) showing increased mean diffusivity in the right caudate streamline. Gaussian smoothing (sigma = 1) was applied on the maps for better visualization.

Figure S5 Interaction effect of groups and fractional anisotropy on mean functional connectivity of the left caudate nucleus.

Table S1 One-sample *t*-test (one-tailed) for the left striatal functional connectivity networks in the healthy control sample

Table S2 Differences in fractional anisotropy and mean diffusivity of white-matter pathway originating from the right caudate in close-to-onset pre-manifest Huntington's disease (pre-HD) compared with healthy controls and far-from-onset pre-HD ($P < 0.05$ based on permutation testing at threshold-free-cluster enhancement family-wise error corrected)

Appendix S1. Supplementary methods.

References

1. Ross CA, Aylward EH, Wild EJ, *et al*. Huntington disease: natural history, biomarkers and prospects for therapeutics. *Nat Rev Neurol* 2014; **10:** 204–216.
2. Tabrizi SJ, Scahill RI, Owen G, *et al*. Predictors of phenotypic progression and disease onset in premanifest and early-stage Huntington's disease in the TRACK-HD study: analysis of 36-month observational data. *Lancet Neurol* 2013; **12:** 637–649.
3. Bohanna I, Georgiou-Karistianis N, Hannan AJ, Egan GF. Magnetic resonance imaging as an approach towards identifying neuropathological biomarkers for Huntington's disease. *Brain Res Rev* 2008; **58:** 209–225.
4. Malejko K, Weydt P, Süßmuth SD, Grön G, Landwehrmeyer BG, Abler B. Prodromal Huntington disease as a model for functional compensation of early neurodegeneration. *PLoS One* 2014; **9:** e114569.
5. Gregory S, Long JD, Klöppel S, *et al*. Testing a longitudinal compensation model in premanifest Huntington's disease. *Brain* 2018; **141:** 2156–2166.
6. Klöppel S, Gregory S, Scheller E, *et al*. Compensation in preclinical Huntington's disease: evidence from the track-On HD study. *EBioMedicine* 2015; **2:** 1420–1429.
7. Skouras S, Falcon C, Tucholka A, *et al*. Mechanisms of functional compensation, delineated by eigenvector centrality mapping, across the pathophysiological continuum of Alzheimer's disease. *Neuroimage Clin* 2019; **22:** 101777.
8. Moretti DV, Pievani M, Pini L, Guerra UP, Paghera B, Frisoni GB. Cerebral PET glucose hypometabolism in subjects with mild cognitive impairment and higher EEG high-alpha/low-alpha frequency power ratio. *Neurobiol Aging* 2017; **58:** 213–224.
9. Lee SE, Sias AC, Kosik EL, *et al*. Thalamo-cortical network hyperconnectivity in preclinical progranulin mutation carriers. *Neuroimage Clin* 2019; **22:** 101751.
10. Seeley WW, Crawford RK, Zhou J, Miller BL, Greicius MD. Neurodegenerative diseases target large-scale human brain networks. *Neuron* 2009; **62:** 42–52.
11. Zhang HY, Wang SJ, Liu B, *et al*. Resting brain connectivity: changes during the progress of Alzheimer disease. *Radiology* 2010; **256:** 598–606.
12. Pini L, Jacquemot C, Cagnin A, *et al*. Aberrant brain network connectivity in presymptomatic and manifest Huntington's disease: a systematic review. *Hum Brain Mapp* 2020; **41:** 256–269.
13. Penney JB Jr, Vonsattel JP, MacDonald ME, Gusella JF, Myers RH. CAG repeat number governs the development rate of pathology in Huntington's disease. *Ann Neurol* 1997; **41:** 689–692.
14. Harrington DL, Rubinov M, Durgerian S, *et al*. Network topology and functional connectivity disturbances precede the onset of Huntington's disease. *Brain* 2015; **138:** 2332–2346.
15. Gorges M, Müller HP, Mayer IMS, *et al*. Intact sensory-motor network structure and function in far from

onset premanifest Huntington's disease. *Sci Rep* 2017; **7:** 43841.
16. Kronenbuerger M, Hua J, Bang JYA, *et al*. Differential changes in functional connectivity of striatum-prefrontal and striatum-motor circuits in premanifest Huntington's disease. *Neurodegener Dis* 2019; **19:** 78–87.
17. Huntington Study Group. Unified Huntington's disease rating scale: reliability and consistency. *Mov Disord* 1996; **11:** 136–142.
18. Tabrizi SJ, Langbehn DR, Leavitt BR, *et al*. Biological and clinical manifestations of Huntington's disease in the longitudinal TRACK-HD study: cross-sectional analysis of baseline data. *Lancet Neurol* 2009; **8:** 791–801.
19. Schobel SA, Palermo G, Auinger P, *et al*. Motor, cognitive, and functional declines contribute to a single progressive factor in early HD. *Neurology* 2017; **89:** 2495–2502.
20. Whitfield-Gabrieli S, Nieto-Castanon A. Conn: a functional connectivity toolbox for correlated and anticorrelated brain networks. *Brain Connect* 2012; **2:** 125–141.
21. Zalesky A, Fornito A, Bullmore ET. Network-based statistic: identifying differences in brain networks. *NeuroImage* 2010; **53:** 1197–1207.
22. Draganski B, Kherif F, Kloppel S, *et al*. Evidence for segregated and integrative connectivity patterns in the human basal ganglia. *J Neurosci* 2008; **28:** 7143–7152.
23. Greene DJ, Marek S, Gordon EM, *et al*. Integrative and network-specific connectivity of the basal ganglia and thalamus defined in individuals. *Neuron* 2019; **105:** 742–758.
24. Ciamei A, Morton AJ. Progressive imbalance in the interaction between spatial and procedural memory systems in the R6/2 mouse model of Huntington's disease. *Neurobiol Learn Mem* 2009; **92:** 417–428.
25. Petrella LI, Castelhano JM, Ribeiro M, *et al*. A whole brain longitudinal study in the YAC128 mouse model of Huntington's disease shows distinct trajectories of neurochemical, structural connectivity and volumetric changes. *Hum Mol Genet* 2018; **27:** 2125–2137.
26. Cabanas M, Bassil F, Mons N, Garret M, Cho YH. Changes in striatal activity and functional connectivity in a mouse model of Huntington's disease. *PLoS One* 2017; **12:** e0184580.
27. Mühlau M, Gaser C, Wohlschläger AM, *et al*. Striatal gray matter loss in Huntington's disease is leftward biased. *Mov Disord* 2007; **22:** 1169–1173.
28. Minkova L, Gregory S, Scahill RI, *et al*. Cross-sectional and longitudinal voxel-based grey matter asymmetries in Huntington's disease. *Neuroimage Clin* 2017; **17:** 312–324.
29. Liu W, Yang J, Burgunder J, Cheng B, Shang H. Diffusion imaging studies of Huntington's disease: a meta-analysis. *Parkinsonism Relat Disord* 2016; **32:** 94–101.
30. Douaud G, Behrens TE, Poupon C, *et al*. In vivo evidence for the selective subcortical degeneration in Huntington's disease. *NeuroImage* 2009; **46:** 958–966.
31. Rosas HD, Tuch DS, Hevelone ND, *et al*. Diffusion tensor imaging in presymptomatic and early Huntington's disease: selective white matter pathology and its relationship to clinical measures. *Mov Disord* 2006; **21:** 1317–1325.
32. Nanetti L, Contarino VE, Castaldo A, *et al*. Cortical thickness, stance control, and arithmetic skill: an exploratory study in premanifest Huntington disease. *Parkinsonism Relat Disord* 2018; **51:** 17–23.
33. Dogan I, Eickhoff CR, Fox PT, *et al*. Functional connectivity modeling of consistent cortical-striatal degeneration in Huntington's disease. *Neuroimage Clin* 2015; **7:** 640–652.
34. Joshi PR, Wu NP, André VM, *et al*. Age-dependent alterations of corticostriatal activity in the YAC128 mouse model of Huntington disease. *J Neurosci* 2009; **29:** 2414–2427.
35. Zullo JM, Drake D, Aron L, *et al*. Regulation of lifespan by neural excitation and REST. *Nature* 2019; **574:** 359–364.
36. Pini L, Manenti R, Cotelli M, Pizzini FB, Frisoni GB, Pievani M. Non-invasive brain stimulation in dementia: a complex network story. *Neurodegener Dis* 2018; **18:** 281–301.
37. Ross OA, Mata IF. Driving genotype treatment options down the right path(way). *Mov Disord* 2019; **34:** 1811–1813.

THE IMPORTANCE OF GREY AND WHITE MATTER

In Multiple Sclerosis

Visit GreyAndWhiteMS.com for more information.

Bristol Myers Squibb™